Quantum transport through circularly coupled triple quantum dots

2007 J. Phys.: Condens. Matter 19 156213

(http://iopscience.iop.org/0953-8984/19/15/156213)

IOP PUBLISHING JOURNAL OF PHYSICS: CONDENSED MATTER

J. Phys.: Condens. Matter **19** (2007) 156213 (12pp) doi:10.1088/0953-8984/19/15/156213

Quantum transport through circularly coupled triple quantum dots

Zhao-Tan Jiang[1] **and Qing-feng Sun**[2]

[1] Department of Physics, Beijing Institute of Technology, Beijing 100081, People's Republic of China
[2] Beijing National Lab for Condensed Matter Physics and Institute of Physics, Chinese Academy of Sciences, Beijing 100080, People's Republic of China

E-mail: jiangzhaotan@bit.edu.cn

Received 22 December 2006
Published 21 March 2007
Online at stacks.iop.org/JPhysCM/19/156213

Abstract

We report a theoretical investigation into the Kondo transport properties of circularly coupled triple quantum dots (QDs), composed of one Coulomb-type QD and two Kondo-type QDs. These two Kondo-type QDs are coupled together to form an Aharonov–Bohm (AB) ring by two channels: the direct coupling t_0 and the indirect one t via a Coulomb-type QD-M; these respectively serve as the continuous and discrete channels for observing the Fano effect. It is particularly interesting that this QD system may be seen as a powerful platform for studying the coexistence and interplay of Kondo, Fano and AB effects. First we study the device conductance in the absence of a magnetic field, and striking competition between t_0 and t is obtained. It is shown that the Kondo-induced conductance peak pattern without direct coupling is completely changed into a new pattern characteristic of one deep Fano-induced valley when t_0 becomes sufficiently strong. Furthermore, we show that the position of the bottom of the Fano valley is determined only by the specific values of the direct and indirect couplings. Then by applying a magnetic field to this QD ring we explore the AB oscillations. It is shown that the phase-locking effect still exists even in the Kondo regime, and the conductance is an even function of the reduced magnetic flux. The AB oscillation pattern becomes very complex for the QD-M level $|\varepsilon_M| \approx 0$ and strong t, t_0 couplings. In addition, the Fano-type valley can be strongly varied by the magnetic field in the AB ring.

1. Introduction

Since the Kondo effect [1–4] was observed in artificial quantum dot (QD) systems, many experimental and theoretical studies have been carried out, first in the single QD system and then extending into the more complex structures with many QDs [5–16]. Obviously, the first

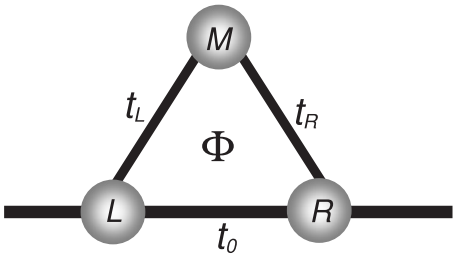

Figure 1. Schematic illustration for a CCTQD device consisting of two coupled Kondo impurities (QD-L and QD-R) connected by direct (t_0) and indirect (QD-M) coupling, penetrated by a magnetic flux Φ.

step in this extension should be the double QD system, which provides us with a flexible tool for studying the double-impurity Kondo problem [17–20]. Previous investigations of the double-impurity Kondo problem have been mainly concentrated on directly coupled double QDs, as well as competition between the Kondo effect and antiferromagnetic coupling. Recently some groups began research on indirectly coupled QDs [21–26]. One representative kind of indirectly coupled double QD was proposed in the pioneering work of Craig *et al* [21], where they devised a double QD system coupled by an open conducting central region and found that the appearance of the zero-bias Kondo anomaly in the curve of conductance versus bias in one QD is closely dependent on the parity of the electron number occupying the other QD. Motivated by this experiment, two theoretical works by Vavilov *et al* [22] and Simon *et al* [23] were carried out to study this indirectly coupled double QD. Recently, Martins *et al* [24] also introduced a simple 'circuit model' to qualitatively study indirectly coupled QDs. Another typical kind of indirectly coupled QD Kondo system are serially coupled triple QDs with two Kondo-type QDs coupled by one intermediate QD; this has been studied recently in [25, 26]. Note that in all these previously studied QD structures only one kind of coupling (direct or indirect) exists. To our knowledge, there is little work dealing simultaneously with both direct and indirect coupling in one QD device.

In this paper, we design one type of circularly coupled triple QDs (CCTQD) in which there coexist both direct and indirect couplings (see figure 1). Hereafter these three QDs are labelled as QD-L, -M and -R, respectively. For simplicity, QD-M can be designed large enough to keep the intradot Coulomb interaction in QD-M negligibly weak. However, QD-L and QD-R, each connected to one normal metal lead, can be viewed as two Kondo impurities when the Coulomb interactions in them are strong enough. These two Kondo impurities are coupled to form a mesoscopic ring through two channels: a direct coupling channel by t_0 and an indirect one by QD-M. In particular, the present CCTQD system has the following characteristics:

(i) Both direct and indirect couplings coexist in CCTQDs, enabling us to study the competition between these two different couplings.
(ii) Two channels, used to couple two Kondo impurities, serve as the continuous channel and the discrete one, which opens up a new way to investigate the Kondo-correlated Fano effect.[3]
(iii) In this special CCTQD one may simultaneously study the Kondo, Fano and Aharonov–Bohm (AB) effects, as well as their interplay.

[3] As an interesting phenomenon, the Fano effect has been extensively investigated both experimentally and theoretically. The necessary condition for observing the Fano effect is the existence of a discrete channel and a continuous one. It is the interference of the electrons through two channels that results in the typical Fano line shape. Originally, it described the line-shape of an optical absorption spectrum.

Recently, Kuzmenko *et al* [27] employed a triangular QD to study the Kondo–AB effect, demonstrating that the conductance as a function of the magnetic field will show sharp enhancement or complete suppression depending on the contact setups. Aharony *et al* [28] investigated the Fano effect in a closed AB interferometer in the *Coulomb* regime. Also, Ladrón de Guevara *et al* [29] studied the quantum transport of parallel-coupled triple QD molecules as well as the Fano effect. All of these recent works were carried out in *triple* QDs, indicating the level of interest in this kind of structure. In the present paper, we use a CCTQD device to investigate the quantum transport properties and Fano effect for two QDs in the *Kondo* regime, and mainly focus attention on the competition between the direct and indirect coupling between two Kondo impurities.

Here we theoretically study the Kondo transport properties through the CCTQD both in the absence and in the presence of a magnetic field. For simplicity we only consider a symmetrical CCTQD device with the energy level $\varepsilon_L = \varepsilon_R \equiv \varepsilon_0$, linewidth function $\Gamma_L = \Gamma_R \equiv \Gamma$ and $t_L = t_R \equiv t$. First of all we show the variations of the linear conductance G versus the QD-M energy level ε_M. It is found that the conductance Kondo peak pattern with $t_0 = 0$ completely evolves into a novel pattern characteristic of a deep Fano-induced valley for sufficiently strong t_0, which clearly shows the competition between direct and indirect coupling. Interestingly, the bottom position of the Fano-induced valley is closely related to both the direct and indirect couplings as $\varepsilon_M^{\min} = t^2/t_0$ in the symmetrical case. Then by applying a magnetic field to the ring we study the AB oscillation of the conductance. As in the usual two-terminal AB system, the conductance G in the Kondo regime also has a phase-locking effect and G is an even function of the reduced magnetic flux ϕ with a period of 2π [30, 31]. In the case of $|\varepsilon_M|/\Gamma \gg 0$ or weak coupling ($t, t_0 \ll \Gamma$), the electron transport is mainly through a first-order tunnelling process and the curve of G versus ϕ is nearly sinusoidal. Otherwise, multiple transmission and reflection processes emerge and the higher order tunnelling processes lead to more complex patterns of the AB oscillations.

The rest of this paper is organized as follows. In section 2 we give the Hamiltonian of the CCTQD system and details of the derivation of the Green's function and the conductance. Before performing a numerical study, in section 3 we perform an analytical analysis to capture some fundamental properties of quantum transport according to the transmission coefficient. Then in section 4 the numerical results are presented. Finally, a brief conclusion is outlined in section 5.

2. Model and formulation

The entire CCTQD system shown in figure 1, composed of three QDs and two adjacent leads, may be modelled by the Anderson Hamiltonian

$$\begin{aligned} H = &\sum_{\alpha k\sigma} \varepsilon_{\alpha k} \hat{c}^{\dagger}_{\alpha k\sigma} \hat{c}_{\alpha k\sigma} + \sum_{\beta\sigma} (\varepsilon_\beta \hat{d}^{\dagger}_{\beta\sigma} \hat{d}_{\beta\sigma} + U_\beta \hat{n}_{\beta\uparrow} \hat{n}_{\beta\downarrow}) \\ &+ \sum_{\sigma} (t_L \hat{d}^{\dagger}_{L\sigma} \hat{d}_{M\sigma} + t_R \hat{d}^{\dagger}_{R\sigma} \hat{d}_{M\sigma} + t_0 \hat{d}^{\dagger}_{L\sigma} \hat{d}_{R\sigma} + \text{H.c.}) \\ &+ \sum_{k\sigma} (V_{kL} \hat{c}^{\dagger}_{Lk\sigma} \hat{d}_{L\sigma} + V_{kR} \hat{c}^{\dagger}_{Rk\sigma} \hat{d}_{R\sigma} + \text{H.c.}), \end{aligned} \tag{1}$$

where $\hat{c}^{\dagger}_{\alpha k\sigma}$ ($\hat{c}_{\alpha k\sigma}$) and $\hat{d}^{\dagger}_{\beta\sigma}$ ($\hat{d}_{\beta\sigma}$) are the electron creation (annihilation) operators in lead-α ($\alpha \in \{L, R\}$) and dot-β ($\beta \in \{L, M, R\}$), respectively; $\hat{n}_{\beta\sigma} \equiv \hat{d}^{\dagger}_{\beta\sigma} \hat{d}_{\beta\sigma}$ indicates the electron number in QD-β with spin σ. Each QD includes a single energy level ε_β and an intradot Coulomb interaction U_β. The interdot coupling between QD-$L(R)$ and QD-M is denoted by

t_L (t_R), while the coupling between QD-$L(R)$ and the left (right) lead is represented by V_{kL} (V_{kR}). In the case of $U_\alpha \to \infty$, the double occupancy in QD-L or QD-R is forbidden, and thus, by using the auxiliary slave-boson operators [18] together with the constraints, the Hamiltonian in equation (1) can be rewritten as

$$\begin{aligned}\hat{H} = &\sum_{\alpha k\sigma} \varepsilon_{\alpha k} \hat{c}^\dagger_{\alpha k\sigma} \hat{c}_{\alpha k\sigma} + \sum_\sigma \varepsilon_M \hat{d}^\dagger_{M\sigma} \hat{d}_{M\sigma} \\ &+ \sum_{\alpha\sigma} (t_\alpha \hat{f}^\dagger_{\alpha\sigma} \hat{b}_\alpha \hat{d}_{M\sigma} + V_{k\alpha} \hat{c}^\dagger_{\alpha k\sigma} \hat{b}^\dagger_\alpha \hat{f}_{\alpha\sigma} + \text{H.c.}) \\ &+ \sum_\sigma (t_{LR} \hat{f}^\dagger_{L\sigma} \hat{b}_L \hat{b}^\dagger_R \hat{f}_{R\sigma} + \text{H.c.}) \\ &+ \sum_{\alpha\sigma} [\tilde{\varepsilon}_\alpha \hat{f}^\dagger_{\alpha\sigma} \hat{f}_{\alpha\sigma} + \lambda_\alpha (\hat{b}^\dagger_\alpha \hat{b}_\alpha - 1)],\end{aligned} \tag{2}$$

where $\tilde{\varepsilon}_\alpha = \varepsilon_\alpha + \lambda_\alpha$ is the Kondo energy level. Also, the Coulomb interaction in QD-M is assumed to be zero. In this slave-boson representation, the creation (annihilation) operator $\hat{d}^\dagger_{\alpha\sigma}$ ($\hat{d}_{\alpha\sigma}$) in QD-α can be expressed as $\hat{d}^\dagger_{\alpha\sigma} = \hat{f}^\dagger_{\alpha\sigma} \hat{b}_\alpha$ ($\hat{d}_{\alpha\sigma} = \hat{b}^\dagger_\alpha \hat{f}_{\alpha\sigma}$) with a boson field operator $\hat{b}_\alpha$ and a pseudofermion field operator $\hat{f}_{\alpha\sigma}$. Within such a method, the intradot Coulomb interaction term is replaced by the constraint

$$\hat{b}^\dagger_\alpha \hat{b}_\alpha + \sum_\sigma \hat{f}^\dagger_{\alpha\sigma} \hat{f}_{\alpha\sigma} = 1, \tag{3}$$

which prevents double occupancy in QD-α. This confinement can be implemented by appending a term $\lambda_\alpha(\hat{b}^\dagger_\alpha \hat{b}_\alpha + \sum_\sigma \hat{f}^\dagger_{\alpha\sigma} \hat{f}_{\alpha\sigma} - 1)$ to H, where λ_α is a Lagrange multiplier to be determined self-consistently. In the following, the slave-boson mean-field approximation is adopted, and the slave-boson operator $\hat{b}_\alpha$ is replaced by a constant number b_α which will be determined self-consistently. Under this approximation, the charge fluctuations around the average $\langle \hat{b}_\alpha(t) \rangle$ are ignored. At low temperatures it can describe the Kondo regime correctly and almost exactly at $T = 0$ limit [18].

Next we study the quantum transport properties through the CCTQD device based on the standard Keldysh non-equilibrium Green's function method [32–35]. The current through the CCTQD is denoted by

$$I_R = \frac{2e}{\hbar} \text{Im} \int \frac{d\varepsilon}{2\pi} \tilde{\Gamma}_R [f_R (G^r_{RR} - G^a_{RR}) + G^<_{RR}], \tag{4}$$

and the linear conductance is

$$G = \frac{2e}{h} \text{Im} \int \text{d}\varepsilon \tilde{\Gamma}_R \frac{dG^<_{RR}(\varepsilon)}{\text{d}V}, \tag{5}$$

where the bias $V = V_L - V_R$ and the right lead bias $V_R = 0$ is assumed to be the energy zero point. $f_{L/R}(\varepsilon) = 1/\{\exp[(\varepsilon - V_{L/R})/K_\text{B}T] + 1\}$ is the Fermi distribution function of the left/right lead, and $\tilde{\Gamma}_\alpha \equiv 2\pi \sum_k \tilde{V}^*_{k\alpha} \tilde{V}_{k\alpha} \delta(\varepsilon - \varepsilon_{\alpha k}) \equiv b^2_\alpha \Gamma_\alpha$ with $\tilde{V}_{k\alpha} \equiv V_{k\alpha} b_\alpha$. $G^r_{\text{nm}}(\varepsilon)$ and $G^<_{\text{nm}}(\varepsilon)$ in equations (4) and (5) are the Fourier transforms of the standard retarded and lesser Green's functions $G^r_{\text{nm}}(t)$ and $G^<_{\text{nm}}(t)$, which are 3×3 matrices with indices $n, m = L, M, R$ for three QDs. For example, the matrix element $G^r_{\text{nm}}(t)$ of the retarded Green's function $\mathbf{G}^r(t)$ is defined as[4]

$$G^r_{\text{nm}}(t) = -\text{i}\theta(t) \langle \{ \hat{f}_{n\sigma}(t), \hat{f}^\dagger_{m\sigma} \} \rangle. \tag{6}$$

All the relevant Green's functions can be solved by using the Dyson equation $\mathbf{G}^r = \mathbf{g}^r + \mathbf{G}^r \mathbf{\Sigma}^r \mathbf{g}^r$ and the Keldysh equation $\mathbf{G}^< = \mathbf{G}^r \mathbf{\Sigma}^< \mathbf{G}^a$. Here $g^r_{\beta\beta}(\varepsilon) = (\varepsilon - \tilde{\varepsilon}_{\beta\sigma} + \text{i}0^+)^{-1}$ is

[4] The spin index can be ignored since the spin-up component always equals the spin-down one.

the exact retarded Green's function of the isolated QD-β, while all the other non-diagonal elements of $\mathbf{g}^r$ are kept at zero. For the lesser self-energy $\mathbf{\Sigma}^<$, there exist only two non-zero matrix elements denoted by $\Sigma^<_{LL}(\varepsilon) = \mathrm{i}\tilde{\Gamma}_L f_L(\varepsilon)$ and $\Sigma^<_{RR}(\varepsilon) = \mathrm{i}\tilde{\Gamma}_R f_R(\varepsilon)$. On the other hand, the retarded self-energy $\mathbf{\Sigma}^r$ can be expressed as

$$\mathbf{\Sigma}^r(\varepsilon) = \begin{pmatrix} -\mathrm{i}\tilde{\Gamma}_L/2, & \tilde{t}_L, & \tilde{t}_0 \\ \tilde{t}_L, & 0, & \tilde{t}_R \\ \tilde{t}_0^*, & \tilde{t}_R, & -\mathrm{i}\tilde{\Gamma}_R/2 \end{pmatrix}, \tag{7}$$

where $\tilde{t}_\alpha = t_\alpha b_\alpha$ and $\tilde{t}_0 = t_0 b_L b_R$. Finally, based on the motion equation of the slave-boson operators together with the constraints (equation (3)), [18] the self-consistent equations for the four undetermined parameters $(\lambda_\alpha, b_\alpha)$ can be given by

$$b_\alpha^2 - \mathrm{i}\sum_\sigma \int \frac{\mathrm{d}\varepsilon}{2\pi} G^<_{\alpha\alpha}(\varepsilon) = 1, \tag{8a}$$

$$\lambda_\alpha b_\alpha^2 = \mathrm{i}\sum_\sigma \int \frac{\mathrm{d}\varepsilon}{2\pi} G^<_{\alpha\alpha}(\varepsilon)(\varepsilon - \tilde{\varepsilon}_\alpha). \tag{8b}$$

3. Analytical discussions

Before numerical study, we first analytically examine the current and the conductance behaviours, as well as the transmission coefficient. Usually, the current flowing through a two-terminal device can be expressed in the typical form [36] $I = (2e/h)\int \mathrm{d}\varepsilon T(\varepsilon)[f_L - f_R]$, where $T(\varepsilon)$ is the transmission coefficient. This transmission coefficient in the present CCTQD device can be derived by substituting $G^{r,a,<}_{RR}$ into equation (4) as

$$T(\varepsilon) = \tilde{\Gamma}_L \tilde{\Gamma}_R |G^r_{RL}|^2. \tag{9}$$

Applying the Dyson equation, we can easily derive the retarded Green's function

$$G^r_{RL}(\varepsilon) = \frac{(\varepsilon - \varepsilon_M)\tilde{t}_0^* + \tilde{t}_L \tilde{t}_R}{(\varepsilon - \varepsilon_M)(\epsilon_L \epsilon_R - |\tilde{t}_0|^2) - \epsilon_L \tilde{t}_R^2 - \epsilon_R \tilde{t}_L^2 - \tilde{t}_L \tilde{t}_R \tilde{t}'} \tag{10}$$

with $\epsilon_L \equiv (\varepsilon - \tilde{\varepsilon}_L + \mathrm{i}\tilde{\Gamma}_L/2)$, $\epsilon_R \equiv (\varepsilon - \tilde{\varepsilon}_R + \mathrm{i}\tilde{\Gamma}_R/2)$, and $\tilde{t}' \equiv 2\,\mathrm{Re}\tilde{t}_0$. From equations (9) and (10) the transmission coefficient is obviously given by

$$T(\varepsilon) = \frac{\tilde{\Gamma}_L \tilde{\Gamma}_R |(\varepsilon - \varepsilon_M)\tilde{t}_0^* + \tilde{t}_L \tilde{t}_R|^2}{|(\varepsilon - \varepsilon_M)(\epsilon_L \epsilon_R - |\tilde{t}_0|^2) - \epsilon_L \tilde{t}_R^2 - \epsilon_R \tilde{t}_L^2 - \tilde{t}_L \tilde{t}_R \tilde{t}'|^2}. \tag{11}$$

In the case of $t_L = t_R = 0$, the CCTQD device is simplified to a serially coupled double QD system, where the transmission coefficient $T(\varepsilon)$ in equation (11) becomes

$$T(\varepsilon) = \frac{\tilde{\Gamma}_L \tilde{\Gamma}_R |\tilde{t}_0|^2}{|\epsilon_L \epsilon_R - |\tilde{t}_0|^2|^2}, \tag{12}$$

which is in agreement with the result obtained by Aono and Eto [20]. Furthermore, in the symmetrical case with $\varepsilon_L = \varepsilon_R \equiv \varepsilon_0$ and $\Gamma_L = \Gamma_R \equiv \Gamma$, $T(\varepsilon)$ can be simplified to

$$T(\varepsilon) = \frac{\tilde{\Gamma}^2 |\tilde{t}_0|^2}{[(\varepsilon - \tilde{\varepsilon}_0)^2 - (|\tilde{t}_0|^2 - \tilde{\Gamma}^2/4)]^2 + \tilde{\Gamma}^2 |\tilde{t}_0|^2}. \tag{13}$$

It is clear that the linear conductance $G(\varepsilon = 0) = (2e^2/h)T(0)$ shows resonant peaks localized at $\tilde{\varepsilon}_0 = \pm\sqrt{|\tilde{t}_0|^2 - \tilde{\Gamma}^2/4}$.

On the other hand, when t_0 is selected to be zero, the transmission coefficient in equation (11) for the symmetrical structure is reduced to

$$T(\varepsilon = 0) = \frac{\tilde{\Gamma}^2\tilde{t}^4}{[\varepsilon_M(\tilde{\varepsilon}_0^2 + \tilde{\Gamma}^2/4) - 2\tilde{\varepsilon}_0\tilde{t}^2]^2 + \tilde{\Gamma}^2\tilde{t}^4} \tag{14}$$

which is the same as the result corresponding to the serially coupled triple QD system, where one resonant peak can be found at [26]

$$\varepsilon_M = 2\tilde{\varepsilon}_0\tilde{t}^2\left(\tilde{\varepsilon}_0^2 + \frac{\tilde{\Gamma}^2}{4}\right)^{-1}. \tag{15}$$

Evidently, the transmission coefficients in both the double and triple QD systems have Lorentz-like characteristic shapes. In fact, the numerator in equation (11) can be decomposed into three parts: $\tilde{\Gamma}_L\tilde{\Gamma}_R|(\varepsilon - \varepsilon_M)\tilde{t}_0^*|^2$, $\tilde{\Gamma}_L\tilde{\Gamma}_R|\tilde{t}_L\tilde{t}_R|^2$, and $\tilde{\Gamma}_L\tilde{\Gamma}_R(\varepsilon - \varepsilon_M)\tilde{t}_L\tilde{t}_R\tilde{t}'$. Here the first and second terms represent electron transport through the QD-M channel and the direct coupling channel, respectively, while the third denotes the coherent component between the two channels. The constructive and destructive interferences plus the two Lorentzian shapes form the Fano-type conductance curves.

Next we put emphasis on the conditions for resonance ($T(0) = 1$, complete transmission) and anti-resonance ($T(0) = 0$, complete reflection), which will help us understand the transport phenomenon more clearly. From equation (11), we can obtain the condition for anti-resonance $|-\varepsilon_M\tilde{t}_0^* + \tilde{t}_L\tilde{t}_R|^2 = 0$, which can be further simplified to $|-\varepsilon_M t_0^* + t_L t_R|^2 = 0$. For real interdot couplings (t_L, t_R, and t_0) the condition becomes

$$\varepsilon_M^{\min} = t_L t_R/t_0, \tag{16}$$

which can be further simplified as $\varepsilon_M^{\min} = t^2/t_0$ for $t_L = t_R = t$. We find that the anti-resonance position $\varepsilon_M^{\min}$, only localized on the $\varepsilon_M^{\min} \geqslant 0$ side, is directly proportional to the indirect couplings (t_L, t_R) and inversely proportional to the direct one (t_0). Very surprisingly, the anti-resonance position is only determined by the bare interdot couplings in such a complex structure with two Kondo-type QDs, and is not affected by the levels ϵ_L and ϵ_R, the temperature T, the Kondo temperature $k_{\mathrm{B}}T_{\mathrm{K}}$ or the Kondo-induced renormalization of the physical parameters. However, when the mesoscopic ring is subject to a magnetic field, the interdot coupling $t_0 = |t_0|\mathrm{e}^{\mathrm{i}\phi}$ may become a complex number, while t_L, t_R and ε_M stay as real numbers. Then the anti-resonance position can appear (only) at the magnetic flux $\phi = n\pi$ ($n = 0, \pm1, \pm2, \ldots$) with $\varepsilon_M^{\min} = (-1)^n t_L t_R/|t_0|$. This indicates that the Fano-induced valley position can be tuned on either side of $\varepsilon_M = 0$ for the integer n. Similarly, from equation (11) the condition of the resonance with $T(0) = 1$ in a symmetrical CCTQD can also be obtained:

$$\varepsilon_M^{\max} = \frac{2\tilde{t}^2(\tilde{\varepsilon}_0 - \tilde{t}_0)}{\tilde{\varepsilon}_0^2 - \tilde{t}_0^2 + \tilde{\Gamma}^2/4}. \tag{17}$$

By comparison with equation (16), we find that the resonance position closely depends on four renormalized physical parameters $\tilde{\varepsilon}_0$, $\tilde{t}$, $\tilde{t}_0$ and $\tilde{\Gamma}$, in sharp contrast to the anti-resonance condition. The resonance position is directly proportional to $\tilde{t}^2$ and decreases with increasing $\tilde{t}_0$. In the case of $t_0 = 0$, we recover the result of the serial triple QDs in equation (15). This should be an effective verification of the validity of the general transmission coefficient in equation (11) and the resonance condition given by equation (17).

4. Numerical results

In this section, we numerically study the quantum transport properties through the CCTQD device in the Kondo regime. For simplicity, we mainly focus on the symmetrical structure,

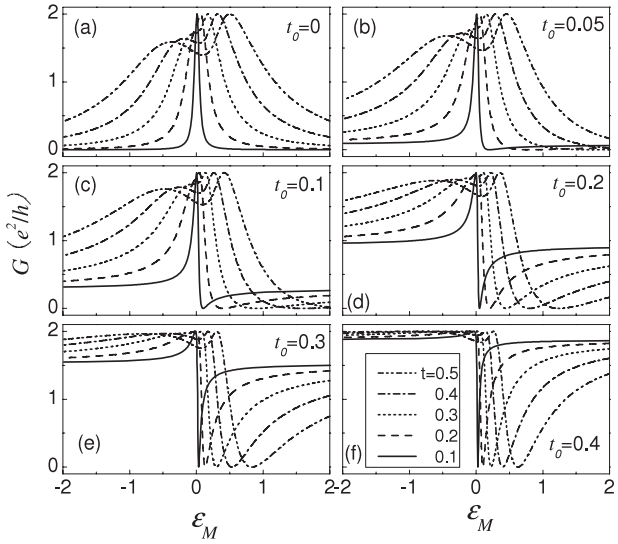

Figure 2. Conductance G versus energy level ε_M of QD-M for different indirect couplings t and direct couplings t_0.

with $\Gamma_L = \Gamma_R \equiv \Gamma = 1$ as the energy unit, the energy level $\varepsilon_L = \varepsilon_R \equiv \varepsilon_0 = -2.3$, and $t_L = t_R = t$. Also, we consider a very low temperature $K_B T = 10^{-6}$.

4.1. Without a magnetic field

To begin with, we consider quantum transport through the CCTQD in the absence of a magnetic field. Figure 2 shows the linear conductance G versus the energy level ε_M of QD-M for different t_0 and t. When $t_0 = 0$, the CCTQD can be reduced to a serially coupled triple QD system, which has been studied in a recent work [26]. The meaningful results for the conductance G can be summarized as (see figure 2(a)):

(1) In the weak coupling case with small t, only one conductance peak is observed at $\varepsilon_M \simeq 0$.
(2) In the large t case, a double peak pattern appears in the conductance curve.

Then, with increasing t_0 from zero, the direct coupling channel is opened and the conductance G exhibits a very different pattern (see figures 2(b)–(f)):

(1) For the weak coupling t, the single conductance peak pattern is inclined to be destroyed, and one deep anti-resonance valley is formed.
(2) For the strong coupling t, first the left peak in the double peak pattern and then the right one is inclined to be submerged, while the deep anti-resonance valley remains.
(3) For a certain t, the deep valley in the conductance curve becomes steeper and its bottom shifts towards zero with the increase in t_0.
(4) For a certain t_0, the valleys are widened and their bottoms are pushed away from zero when t becomes large.
(5) For $t \neq 0$, the asymmetrical double peaks are pushed away from $\varepsilon_M = 0$ with increasing t, while they approach the $\varepsilon_M = 0$ position from two opposite directions with increasing t_0.

How do these phenomena come into being? Clearly, when the direct coupling t_0 is zero, the system is a serially coupled triple QD system. In this case, the electron transport through

the system must pass through the QD-M channel. When the direct coupling t_0 becomes non-zero, another channel of t_0 is opened. Obviously, with further increase in t_0 more electrons are directly transported from QD-L to QD-R through the t_0 channel, and this channel is dominant in the limit $t_0 \gg t$. Therefore in the area $|\varepsilon_M| \gg 0$ the conductance is highly enhanced due to the switching on of the new t_0 channel (see figure 2(f)). By observing the solid curves corresponding to the weak t (=0.1) case, the conductance G shows the visible enhancement that will submerge the original single conductance peak with the opening of the direct channel t_0. In the meantime, a narrow, deep valley emerges, which results from destructive interference between the two channels. At certain values of t and t_0, an obviously asymmetrical line shape appears, which can be attributed to the Fano effect (see figures 2(c)–(f)). As we see, for strong t coupling, the t_0-channel-induced enhancement of conductance will first submerge the low (left) peak and then the high (right) one in the double peak pattern. Nevertheless, the Fano-induced valley is always observed because of the destructive interference between the two channels. The evolution from the single or double peak pattern ($t_0 = 0$) to the deep valley pattern ($t_0 = 0.4$) clearly depicts the competition process between the direct and indirect coupling of the two Kondo impurities.

In the following we consider the bottom of the Fano valley (the anti-resonance position) and the conductance peak (the resonance position). As given by equation (16), in the symmetrical case the anti-resonance position ($\varepsilon_M^{\min} = t^2/t_0$) depends only on t and t_0. It is a universal relation independent of the bare QD energy level $\varepsilon_{L,R}$ and other related parameters, e.g. $\Gamma_{L,R}$ and the temperature. This means that the shape and position of the Fano-induced conductance valley are mainly determined by both direct and indirect coupling. It is shown in figure 2 that the bottom position increases with increasing t and decreases with increasing t_0, in agreement with equation (16). This clearly demonstrates the validity of this simple criterion, which is surprising due to its concise form in so complex a CCTQD system. Physically, this anti-resonance describes the completely destructive interference between two channels, while the resonance describes the completely constructive one. Due to the renormalization of the physical parameters in equation (17), the variation of the resonance position shows a more complex pattern than that of the anti-resonance. Qualitatively, we can find that the two conductance peaks with $t \neq 0$ are shifted away from (towards) the position $\varepsilon_M = 0$ with the increase in the indirect (direct) coupling, as presented in figure 2.

An important physical parameter in the Kondo effect is the Kondo energy level $\tilde{\varepsilon}$ (in the symmetrical case, $\tilde{\varepsilon}_L = \tilde{\varepsilon}_R \equiv \tilde{\varepsilon}$). In figure 3, we show the variations of the Kondo level $\tilde{\varepsilon}$ as a function of ε_M of QD-M for different couplings t and t_0. When t_0 is chosen to be 0, the Kondo level $\tilde{\varepsilon}$ has one high peak and one gentle valley, and the bottom of the valley can be lower than zero in the strong t case (see figure 3(a)). Further, we can see that when t is very weak (e.g. $t = 0.1$ (solid curves in figure 3)), the Kondo level $\tilde{\varepsilon}$ is quite small for all values of ε_M and t_0, which is different from the case for $t_0 = 0$ where $\tilde{\varepsilon}$ is affected by t (figure 3(a)). For a fixed t, the increase in t_0 certainly strengthens the direct coupling channel of the two Kondo impurities. It will induce a slight increase in the Kondo level, which can be found by a thorough comparison figure 3(a) with figure 3(f). It also can be found that the gentle valley with $t_0 = 0$ is suppressed by the opening of the direct coupling channel and it is inclined to completely disappear when t_0 becomes strong, because the opening of the direct coupling channel can strengthen the co-tunnelling processes and thus enhance the Kondo temperature $k_B T_K$.

Next we carry out more detailed research on the influence of the direct coupling t_0. Figure 4(a) shows the case of $t = 0$, where the conductance initially increases from 0 to $2e^2/h$ (unitary limit) and then decreases, consequently forming one peak centred at $t_0 = (\varepsilon_0^2 + \Gamma_0^2/4)^{1/2} \approx 0.5$, which can be readily obtained from equation (13). Figures 4(b)–(f)

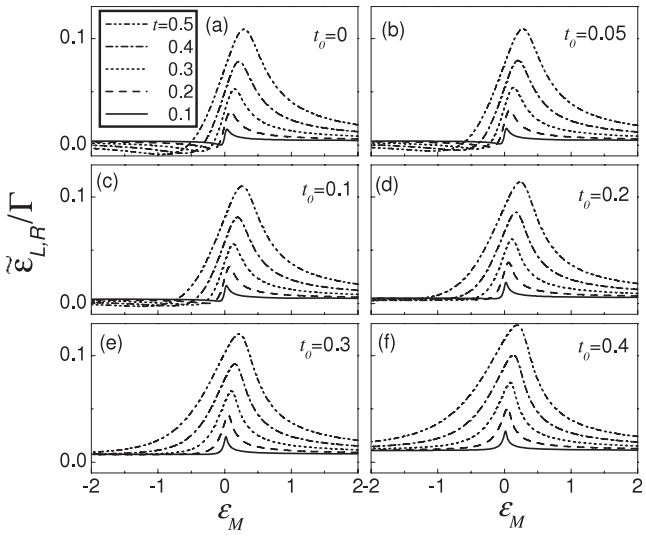

Figure 3. Kondo energy levels in QD-L or QD-R versus energy level ε_M of QD-M for different direct and indirect couplings.

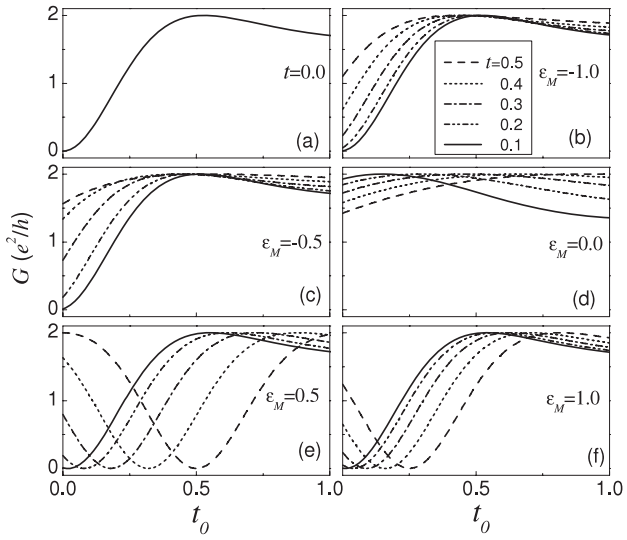

Figure 4. Conductance G versus the direct coupling t_0 between QD-L and QD-R for different indirect couplings t and QD-M energy levels ε_M.

show the conductances through the CCTQD as a function of t_0 for non-zero t and different ε_M. In the case of small t (e.g. $t = 0.1$), the conductances are very similar to that of $t = 0$, except for that of $\varepsilon_M \approx 0$ (figure 4(d)). However, for large t (e.g. $t = 0.5$), an apparent difference appears. In particular, there exists an anti-resonance conductance valley on the side of $\varepsilon_M > 0$ but not on the side of $\varepsilon_M < 0$. The bottoms of the valleys are shifted away from zero as t increases (see figures 4(e) and (f)). This phenomenon can be explained fully according to the criterion denoted by equation (16), which may be rewritten as $t_0^{\min} = t^2/\varepsilon_M$.

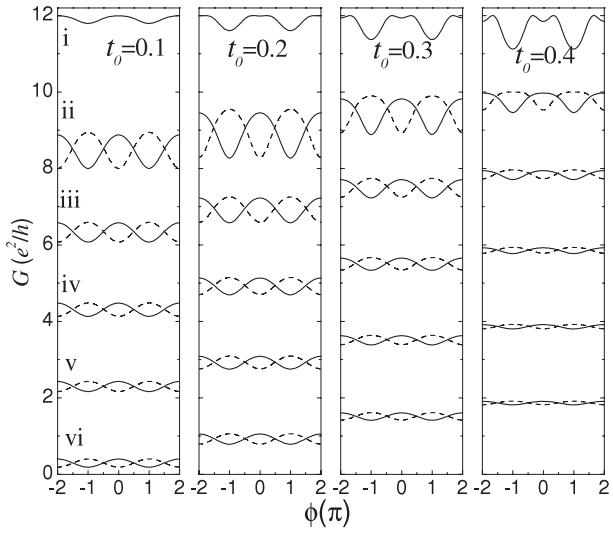

Figure 5. Conductance oscillations as a function of the reduced magnetic flux ϕ at $t = 0.1$. For clarity, the conductances are classified into six groups according to the energy levels: (i) $|\varepsilon_M| = 0.0$, (ii) 0.1, (iii) 0.2, (iv) 0.3, (v) 0.4 and (vi) 0.5, and then increased by different values 10, 8, 6, 4, 2 and 0, respectively. The conductances corresponding to $-|\varepsilon_M|$ and $|\varepsilon_M|$ are plotted by solid and dashed lines, respectively.

4.2. With magnetic field

In what follows, we turn to the influences induced by the magnetic field on the transport properties through the CCTQD ring. Notably, this CCTQD is of peculiar significance because of the coexistence of three kinds of classical effect—the Kondo, Fano and AB effects—as well as two kinds of QDs—Kondo-type QDs (QD-L and QD-R) and the usual QD (QD-M). Our investigations are carried out in both the weak (see figure 5) and the strong (see figure 6) indirect coupling cases.

In figure 5 we show the conductance G versus the reduced magnetic flux ϕ with $t = 0.1$ for different t_0 and ε_M. Three main characteristics can be seen:

(i) As usual, the conductance G in the Kondo regime also oscillates with a period of 2π, and is an even function about ϕ. The closed CCTQD AB ring is a two-terminal system and should have a phase-locking effect due to time-reversal symmetry and current conservation [30, 31].
(ii) G oscillates in phase on either side of $|\varepsilon_M| \approx 0$, while the conductances corresponding to $\varepsilon_M \gg 0$ and $\varepsilon_M \ll 0$ oscillate in the opposite phase. This means that an abrupt phase jump π occurs when ε_M passes through the Fermi energy 0 [31].
(iii) In the area of $|\varepsilon_M| \gg 0$ or in the weak t, t_0 coupling case, G shows a simple and nearly sinusoidal oscillation, which means that the first-order tunnelling process dominates.

However, in the case of $|\varepsilon_M| \approx 0$ and large t_0, the curve G–ϕ shows a complex pattern. This is because both the approach of $\varepsilon_M \to 0$ and the increase of t_0 will promote the occurrence of multiple transmission and reflection processes in the CCTQD AB ring.

Then we consider the AB conductance oscillations in the relatively strong t (=0.3) case (see figure 6). At first glance we may immediately recognize the distinct changes differing from the weak case in figure 5. The original simple oscillation behaviours with $t = 0.1$ have

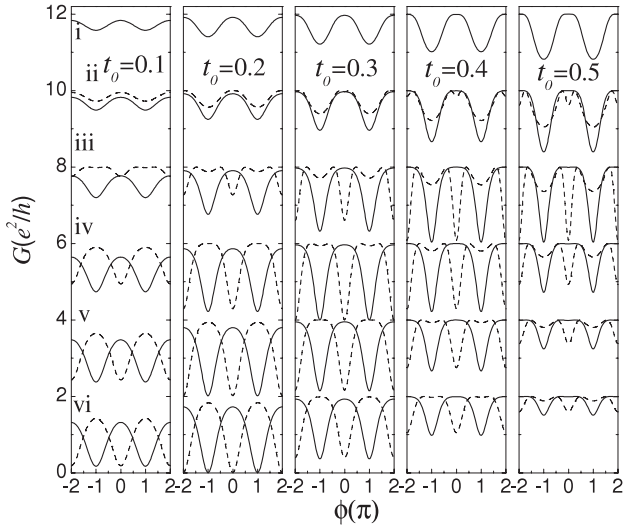

Figure 6. Conductance oscillations as a function of the reduced magnetic flux ϕ at $t = 0.3$. For clarity, the conductances are classified into six groups according to the energy levels: (i) $|\varepsilon_M| = 0.0$, (ii) 0.1, (iii) 0.2, (iv) 0.3, (v) 0.4 and (vi) 0.5, and then increased by different values 10, 8, 6, 4, 2 and 0, respectively. The conductances corresponding to $-|\varepsilon_M|$ and $|\varepsilon_M|$ are plotted by solid and dashed lines, respectively.

been destroyed and then one more complex pattern appears. Most of the curves plotted in figure 6 become non-sinusoidal except for those with small coupling (e.g. $t_0 = 0.1$) and a large QD-M energy level (e.g. $\varepsilon_M = \pm 0.5$). This is a result of the multiple transmission and reflection processes taking place with large probability when t becomes very strong. However, no matter what changes in the oscillation patterns of the conductances, the period of 2π and the even parity about ϕ are still preserved. This is the universal behaviour for the two-terminal AB system, and it is independent of the specific physical parameters such as ε_M, t, t_0 and so forth. Notably, the amplitude of the AB oscillation in the strong t case is very large, and can almost reach the unitary limit $2e^2/h$. This means that the system can be tuned from resonance to anti-resonance and vice versa by changing the reduced magnetic flux ϕ. That is to say, the Fano valley can be varied by the magnetic field. In the zero magnetic field case, the Fano valley is always on the right of the peak with $\varepsilon_M > 0$ (see figure 2). However, by applying a magnetic field, the Fano valley can be moved to the left of the peak (not presented here).

5. Conclusion

In conclusion, we have studied the Kondo transport properties of a circularly coupled triple QD device in both the absence and presence of a magnetic field. In this CCTQD system Kondo, Fano and AB effects coexist, which enables one to simultaneously investigate these three effects as well as their interplay. First we presented the conductances without the magnetic field to study the competition between the direct and indirect channels, and thus the Kondo and Fano effects. It was shown that the conductance peak patterns without direct coupling are changed into new patterns characteristic of one deep Fano-type valley for sufficiently strong direct coupling, and the position of the bottom of the Fano valley is only determined by these two kinds of coupling as $\varepsilon_M^{\min} = t^2/t_0$. Secondly we considered the presence of a magnetic field to investigate the AB oscillations. It is shown that in the Kondo regime the conductance

is still an even function of the reduced magnetic flux with period 2π. The amplitude of the AB oscillation can be quite large in the strong coupling case. Moreover, it is shown that the Fano valley can be tuned on either side of $\varepsilon_M = 0$ by the magnetic field.

Acknowledgments

We gratefully acknowledge financial support from the NSFC under grant nos 10547105, 10604005, 90303016, 10474125 and 10525418; and the Chinese Academy of Sciences. Z-T also acknowledges the support from the Excellent Young Scholars Research Fund of Beijing Institute of Technology (No. 2006Y0713).

References

[1] Hewson A C 1993 *The Kondo Problem to Heavy Fermions* (Cambridge: Cambridge University Press)
[2] Kondo J 1964 *Prog. Theor. Phys.* **32** 37
[3] Ng T K and Lee P A 1988 *Phys. Rev. Lett.* **61** 1768
[4] Meir Y, Wingreen N S and Lee P A 1993 *Phys. Rev. Lett.* **70** 2601
[5] Goldhaber-Gordon D, Shtrikman H, Mahalu D, Abusch-Magder D, Meirav U and Kastner M A 1998 *Nature* **391** 156
[6] Cronenwett S M, Oosterkamp T H and Kouwenhoven L P 1998 *Science* **281** 540
[7] Van der Wiel W G, Franceschi S D, Fujisawa T, Elzerman J M, Tarucha S and Kouwenhoven L P 2000 *Science* **289** 2105
[8] Sasaki S, Franceschi S D, Elzerman J M, Van Der Wiel W G, Eto M, Tarucha S and Kouwenhoven L P 2000 *Nature* **405** 764
[9] Ji Y, Heiblum M, Sprinzak D, Mahalu D and Shtrikman H 2000 *Science* **290** 779
[10] Nordlander P, Pustilnik M, Meir Y, Wingreen N S and Langreth D C 1999 *Phys. Rev. Lett.* **83** 808
[11] Zhang P, Xue Q K, Wang Y and Xie X C 2002 *Phys. Rev. Lett.* **89** 286803
[12] Luo H G, Xiang T, Wang X Q, Su Z B and Yu L 2004 *Phys. Rev. Lett.* **92** 256602
[13] Hu H, Zhang G M and Yu L 2001 *Phys. Rev. Lett.* **86** 5558
[14] Sun Q F, Guo H and Lin T H 2001 *Phys. Rev. Lett.* **87** 176601
[15] Jayaprakash C, Krishna-murthy H R and Wilkins J W 1981 *Phys. Rev. Lett.* **47** 737
[16] Jones B A, Varma C M and Wilkins J W 1988 *Phys. Rev. Lett.* **61** 125
[17] Jeong H, Chang A M and Melloch M R 2001 *Science* **293** 2221
[18] Aguado R and Langreth D C 2000 *Phys. Rev. Lett.* **85** 1946
[19] López A, Aguado R and Platero G 2002 *Phys. Rev. Lett.* **89** 136802
[20] Aono T and Eto M 2001 *Phys. Rev.* **63** 125327
[21] Craig N J, Taylor J M, Lester E A, Marcus C M, Hanson M P and Gossard A C 2004 *Science* **304** 565
[22] Vavilov M G and Glazman L I 2005 *Phys. Rev. Lett.* **94** 086805
[23] Simon P, López R and Oreg Y 2005 *Phys. Rev. Lett.* **92** 086602
[24] Martins G B, Büsser C A, Al-Hassanieh K A, Anda E V, Moreo A and Dagotto E 2006 *Phys. Rev. Lett.* **96** 066802
[25] Büsser C A, Moreo A and Dagotto E 2004 *Phys. Rev.* B **70** 035402
[26] Jiang Z T, Sun Q F and Wang Y P 2005 *Phys. Rev.* B **72** 045332
[27] Kuzmenko T, Kikoin K and Avishai Y 2006 *Phys. Rev. Lett.* **96** 046601
[28] Aharony A, Entin-Wohlman O, Otsuka T, Katsumoto S, Aikawa H and Kobayashi K 2006 *Phys. Rev.* B **73** 195329
[29] Ladrón de Guevara M L and Orellana P A 2006 *Phys. Rev.* B **73** 205303
[30] Buttiker M 1986 *Phys. Rev. Lett.* **57** 1761
[31] Hackenbroich G 2001 *Phys. Rep.* **343** 463
[32] Haug H and Jauho A P 1998 *Quantum Kinetics in Transport and Optics of Semiconductor* (Berlin: Springer)
[33] Chou K C, Su Z B, Hao B L and Yu L 1985 *Phys. Rep.* **118** 1
[34] Meir Y and Wingreen N S 1992 *Phys. Rev. Lett.* **68** 2512
[35] Jauho A P, Wingreen N S and Meir Y 1994 *Phys. Rev.* B **50** 5528
[36] Datta S 2004 *Electronic Transport in Mesoscopic Systems* (Cambridge: Cambridge University Press)